FATIGUE TESTING OF DIAMOND-SHAPED SPECIMENS

Alan R. Pelton, Xiao-Yan Gong, and Tom Duerig

Nitinol Devices & Components, 47533 Westinghouse Drive, Fremont CA 94539

ABSTRACT
This study quantifies the cyclic deformation behavior of superelastic Nitinol in order to calculate design safety factors for medical devices. Displacement-controlled fatigue testing was performed on stent-like devices that were laser-cut from microtubing, shape set and electropolished. Fatigue strains were calculated from displacements with non-linear FEA methods. Fatigue data were collected from –4% to +4% mean strain and oscillating strains of 0.07% to 3% for a maximum of ten million cycles. Contrary to that observed in conventional engineering materials, the magnitude of the mean strain does not limit the fatigue life. Rather, the results demonstrate that the oscillating strain amplitude is the main contributor to fatigue behavior. Increased fatigue life was observed for mean strains above about 1.5%. The data are analyzed with finite element computations and are illustrated with strain-cycle and constant-life graphs.

KEYWORDS
Fatigue, Nitinol, Coffin-Manson, mean strain, FEA

INTRODUCTION
Several researchers investigated the cyclic failure of NiTi alloys for different specimen shapes such as bars, wires, and plates. In general, Nitinol does extremely well in strain- or displacement-controlled fatigue, but does less well in stress-controlled fatigue environments. Nitinol crack-growth rates were measured to be faster with lower fatigue threshold values than observed in conventional engineering alloys such as Ti-6Al-4V or stainless steel [1, 2]. Furthermore, martensitic Nitinol was found to have higher fatigue-crack thresholds slower crack-growth rates compared to stable austenite and superelastic austenite [1, 3, 4]. Fatigue data have also been characterized for rotary bending [5, 6] and uniaxial fully reversed loading [3, 7].

Many of the earlier studies cited above [1, 3, 4, 7] were conducted on fully annealed Ni-Ti alloys that were austenite or martensite at the test temperature. Whereas these initial studies provide tremendous insight into baseline fatigue properties, it is also well known that thermomechanical processing can greatly affect fatigue behavior in engineering materials. Consequently, to gain a keener understanding of the fatigue performance of modern Nitinol medical devices it is imperative that the test program adopts the following conditions:

- comparable sample configurations
- comparable thermomechanical processing
- comparable metallurgical texture
- comparable loading modes
- comparable analytical methods

Recently, several researchers investigated the effects of mean and alternating strain on the fatigue behavior of superelastic Nitinol and observed that the oscillating strain has a greater effect on fatigue life than the mean strain [8-11]. This is an extremely important finding that is contrary to that observed in conventional engineering materials [12] and may provide greater latitude for safe medical device design with Nitinol. Despite the consensus findings, however, the details of these recent studies differ considerably. For example, Tabanli, *et al.* [8] investigated the uniaxial fatigue of Nitinol microtubing with an A_f of about –5˚C with tensile mean strains up to 9% at an alternating strain of approximately 0.2% tested at room temperature (approximately 25˚C difference). Their results are certainly credible, but the samples were not subjected to stent-like processing and the loading forces were in the longitudinal (tensile) rather than the circumferential (multiaxial) tube direction as experienced by stents *in vivo*. Furthermore, their study emphasized the difficulty of testing tubing samples as two of their five samples

experienced grip failure. Tolomeo, *et al.* [9] investigated the fatigue properties of "unzipped" stents after laser cutting and processing, but applied "pull" forces rather than "push" forces; i.e., the maximum principal strains were on the inside of the stent strut rather than the outside. This approach is overly cautious and does not represent the intended physiological applications. Kugler, *et al.* [10] studied laser machined stent-like test samples from Nitinol microtubing but also applied the tensile fatigue deformation to the inside of the strut. The advantage of their study was that they had multiple home-built fatigue testers so that they could run to over 400 million cycles. Harrison and Lin [10] used a "V" test sample based on their stent design and applied the correct "push" loading conditions. However, their data seems to be extremely optimistic compared to other studies; this may possibly be due to out-of-plane deformation or inaccuracies in strain calculation. As a final comment, all of the above investigations based their conclusions on very few data points focused on specific environment conditions.

The focus of the present study was to quantify the effects of strain on the cycles to failure of fully processed Nitinol stent-like testing elements with an A_f of 30˚C. Testing was performed at 37˚C on dedicated fatigue-testing equipment with both push and pull forces to compare maximum principal strains on opposite sections of the strut arms. Fatigue data were collected up to ±4% mean strain and from 0.07% to 3% half alternating strain for a maximum of ten million cycles or an equivalent implant period of approximately 8 months. The rationale for suspending the tests at ten million cycles was to obtain higher numbers of tests out to a reasonable limit rather than to obtain only a few data points at 400 million cycles, the equivalent of ten years of human heart beats. Furthermore, it is a well-accepted and reasonable practice to define an endurance limit at 10^7 cycles [12].

MATERIALS, EXPERIMENTAL PROCEDURES, AND FEA

Diamond stent-like test specimens were laser machined from Nitinol tubing (4.67mm OD with 0.38mm wall) and were shape set so that the arms were aligned in the same manner as stent struts. The samples were surface processed, including electropolishing, similar to stents. Tabs at the top and bottom were designed to provide precise alignment, structural stability, elimination of buckling, and secure gripping during testing. Three samples were tested from each processing lot to ensure an A_f = 26-32˚C.

An EnduraTec ELF/3200 series desktop test system with an integrated break detection system was used to perform the fatigue tests. Up to four samples were tested simultaneously at a frequency of 50Hz. Figure 1 shows the samples loaded into the customized fixture. Since alignment is critical for uniform strain distribution, mounted samples were visually setup and then checked with an external laser micrometer to detect out-of-plane motion. No evidence of buckling was observed for these samples. An environmental chamber, which consists of a temperature controller, an air-heating fan, and thermocouple, was used to maintain the 37˚C test temperature. Once the tests were fully setup, a single load-displacement cycle is recorded to ensure that the parameters are correctly chosen and that the samples are properly fixtured [13]. The diamond-shaped samples were run under displacement-controlled conditions to failure or to a maximum of 10 million cycles.

ABAQUS/Standard version 6.2-1 Finite Element Analysis (FEA) package, in combination with the user-defined material subroutine UMAT/Nitinol-3D version 4.1-2, was used to calculate the stress and strain fields in the samples (see references 13-16 for applications of the codes). Due to symmetry considerations, only a quarter of the specimen is required for the analyses. Symmetrical boundary conditions are enforced at the symmetry surfaces. A single node is fixed in the direction perpendicular to the diamond surface to prevent out-of-plane rigid body translation. Constant displacement is applied at the upper edge of the model to load the diamond. Typical strain contours of the sample under simulated push (2a) and pull (2b) conditions are shown in Figure 2. The peak maximum principal strain locations determined by FEA are illustrated on the figures.

The FEA model was validated with load-deflection curves from the test samples that were pulled to a set displacement, pushed to the same absolute deflection and then released back to the original neutral position. The load-deflection experimental results agree very well with the FEA prediction, as shown in Figure 3. This agreement is comparable to that observed for stent and other medical device modeling (see for example, references 14-17). Note that these curves are non-symmetric in load; for example, a 6 mm deflection in the pull direction requires 3 N force; whereas for the same displacement in the push direction, the force is just over 2 N. These force differences are due to geometry factors as well as the non-linear behavior of Nitinol.

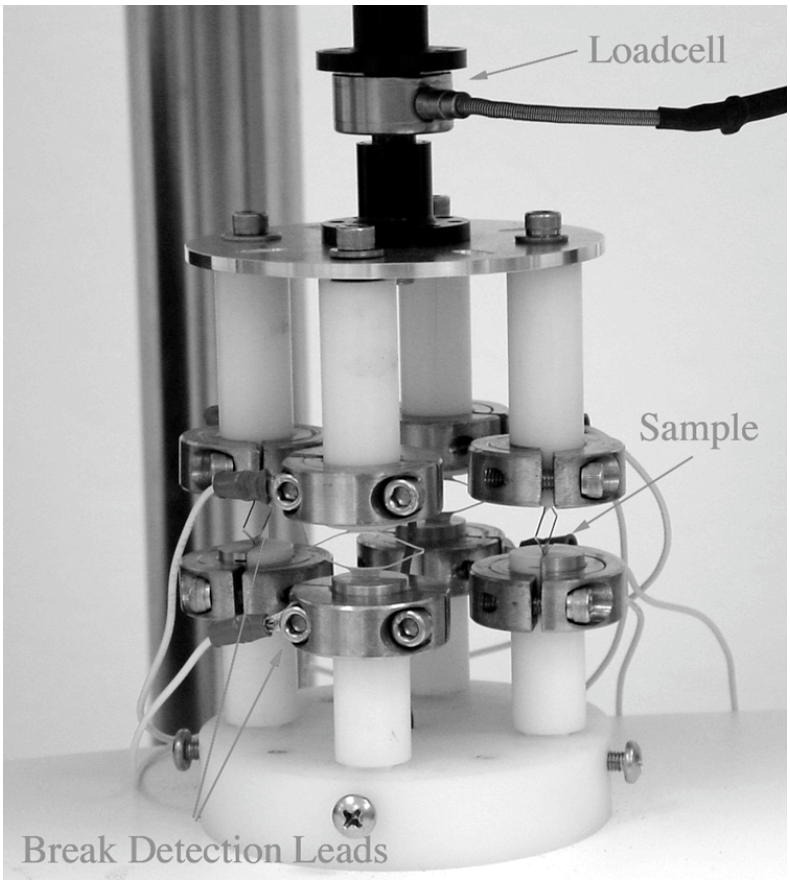

Figure 1: Image of the diamond-fatigue set up on the EnduraTec ELF System which includes four sample holders, loadcell, and break-detection system.

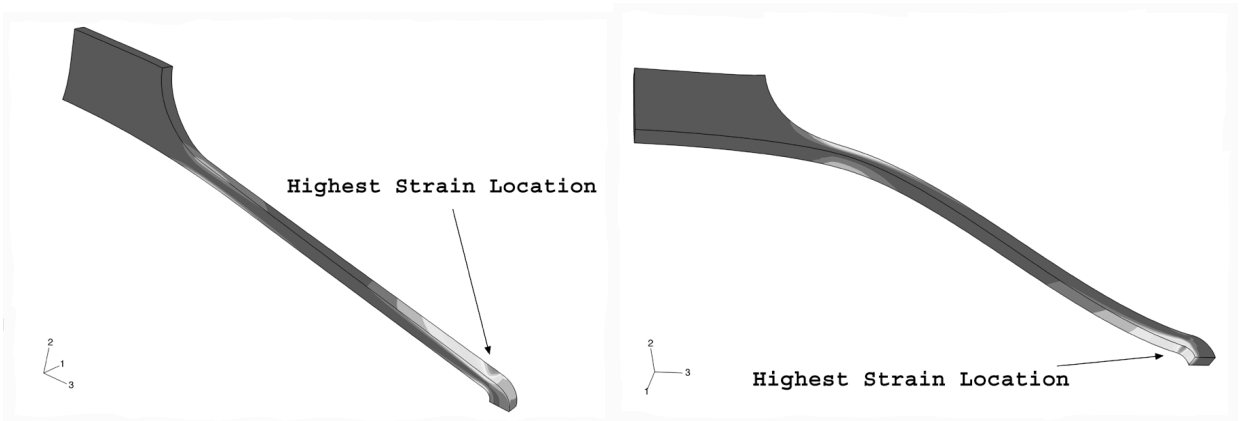

(a) (b)

Figure 2: FEA strain contours of the diamond sample that illustrate the highest strain conditions on the diamond samples under conditions of push ("compressive") (a) and pull ("tensile") (b) forces.

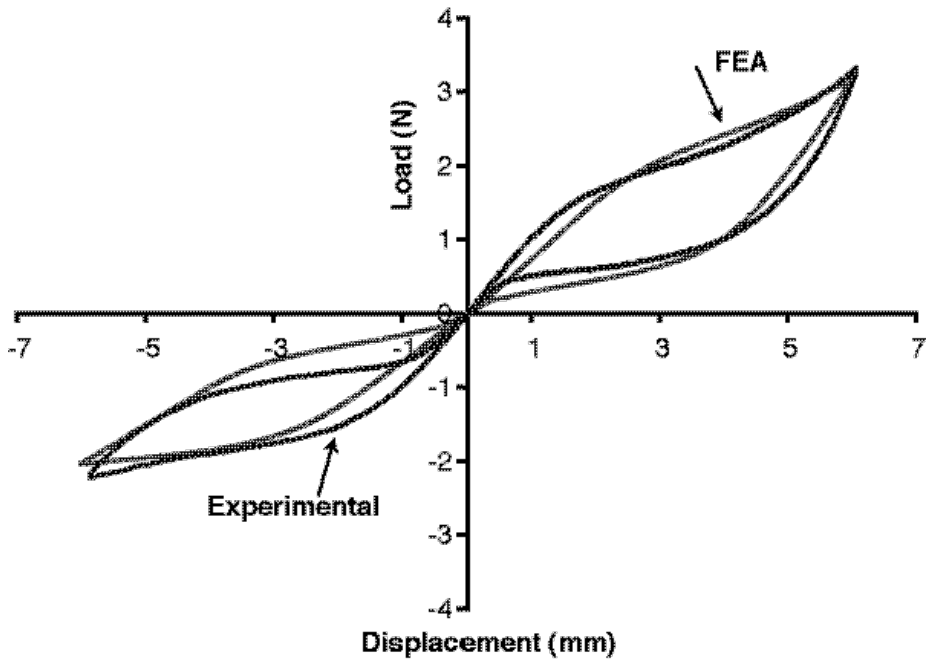

Figure 3: Comparison of the load-deflection experimental results with the FEA model with both pull (quadrant 1) and push (quadrant 3) data.

RESULTS AND DISCUSSION

Strain-Cycle Analysis

The experimental deflections, FEA calculated strains, and cycle counts from 432 samples were evaluated in this study. Figure 4 shows the half-alternating strain *vs*. cycle count data for conditions of zero-mean strain. A trendline is drawn through the low-cycle data ($N<10^5$) corresponding to a Coffin-Manson analysis [12]. An exponent of –0.41 was determined for these data, which compares well with a value of –0.42 determined by Tolomeo, *et al*. for a mean strain of 0.5% [8]. Melton and Mercier found an exponent of –0.32 for fully annealed samples with an M_s of 30˚C, tested at 20˚C [6]. These exponent differences between the older [6] and more recent stent-based studies are not unexpected and point to the effects of thermomechanical processing and deforming phase on cyclic deformation.

A trendline was also drawn through the high cycle data ($N>10^5$) for illustrative purposes. According to these high-cycle data, the 10^7-cycle zero-mean strain endurance limit is 0.4% strain. Note that several samples that were cycled between 0.2% and 0.6% alternating strain survived the 10^7 cycle tests; these data are marked with arrows to indicate runout. It is also interesting to compare these data to the wire rotary bend data [5,6]. Although the processing and test conditions differ slightly between the two wire-based investigations, they both obtained zero-mean endurance limits of approximately 0.7% strain. Under these loading conditions the outer surfaces of the wires experience maximum tension and maximum compression during each revolution. Consequently, the applied strain is alternately cycled through zero, allowing full recovery of the stresses. For the present diamond samples at zero-mean strain, the tensile and compressive stresses alternate from the bottom to the top of the diamond arms; however, the elements do not necessarily experience full tensile and compressive stresses. An SEM analysis of the broken diamond samples showed that fatigue cracks always initiate on the inner surface of the arms under these zero-mean conditions, as shown in Figure 5. Note that the fracture occurred at the location predicted by FEA (Figure 2b). Figure 5b is a higher magnification image of the fracture surface that indicates that the initiation site was on the inside (tensile) of the diamond. This difference between push and pull behavior in the current study is likely due to the slight differences in surface finish on the inside and outside of the diamond specimens. Mechanical and electrochemical surface processing techniques are better able to remove minor surface defects from external surfaces created by laser processing and expansion compared with those on internal surfaces. Indeed, a parallel study of the effects of surface finish on fatigue behavior showed conclusively that less optimal surface finishes led to lower fatigue life [18].

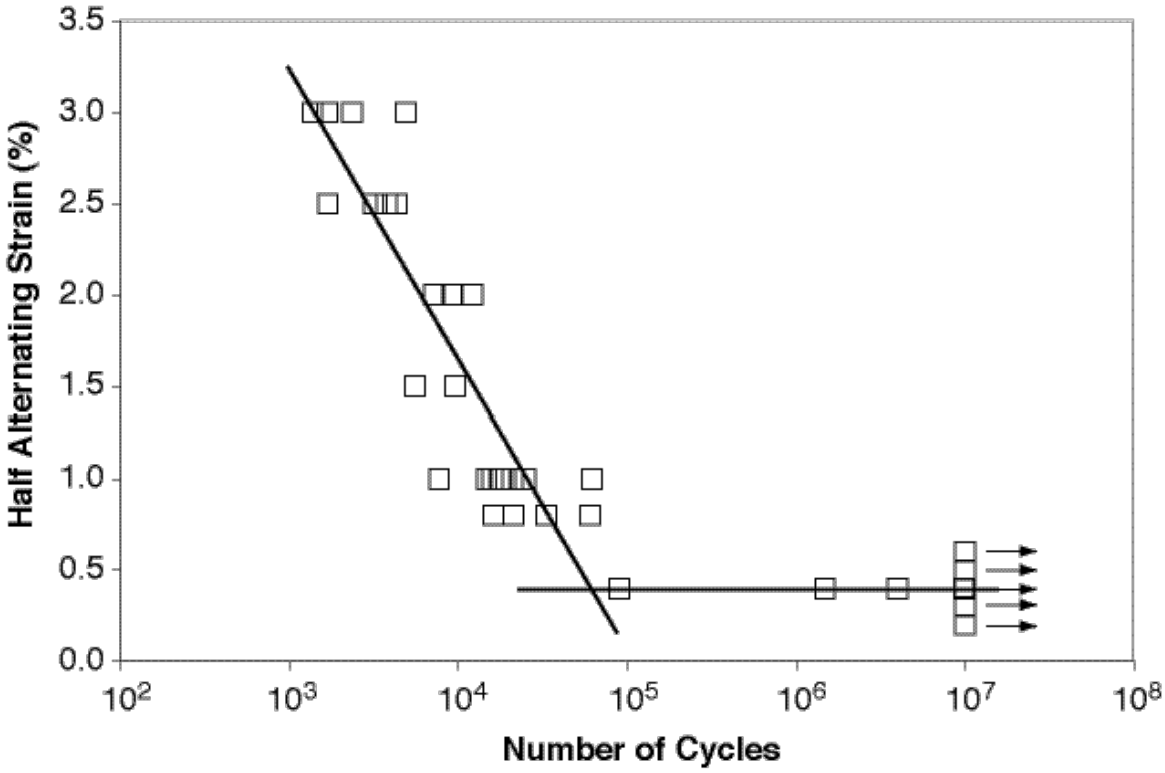

Figure 4: Strain-cycle data from the diamond-shaped samples that were cycled to failure at zero-mean strain as a function of half-amplitude strain. Trendlines through the low-cycle (Coffin-Manson behavior) and high-cycle fatigue data are drawn for illustrative purposes. The samples at 10^7 cycles did not fracture. The endurance limit from these data is 0.4%.

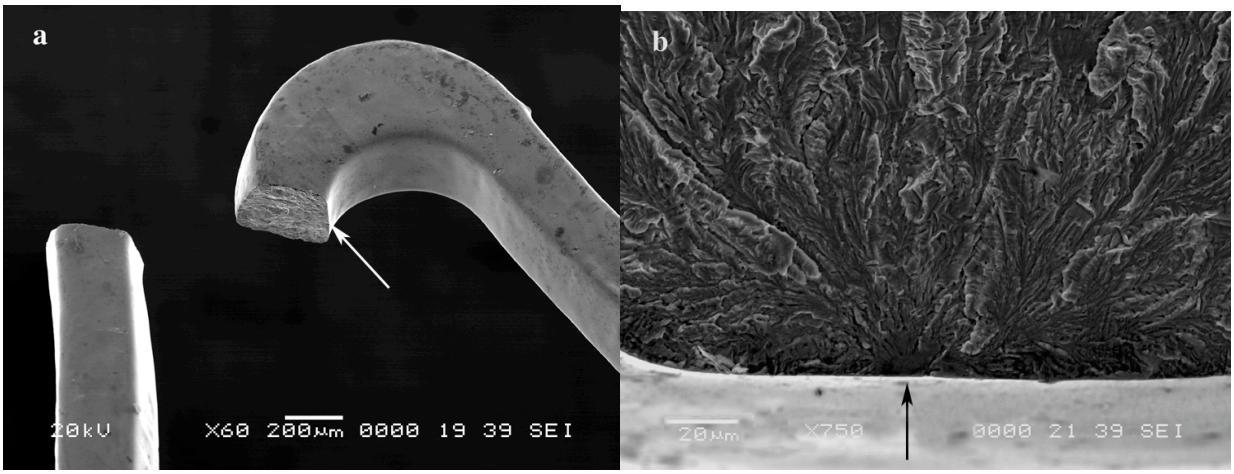

Figure 5: SEM images of a diamond fatigue specimen that failed at 9.8 million cycles at zero mean strain and 0.4% half alternating strain. Figure 5a illustrates that the high strain area predicted by FEA (Figure 2b); the white arrow indicates the initiation site. Figure 5b shows a higher magnification image of the fracture surface on the inside surface of the diamond where the initiation site is marked with a black arrow.

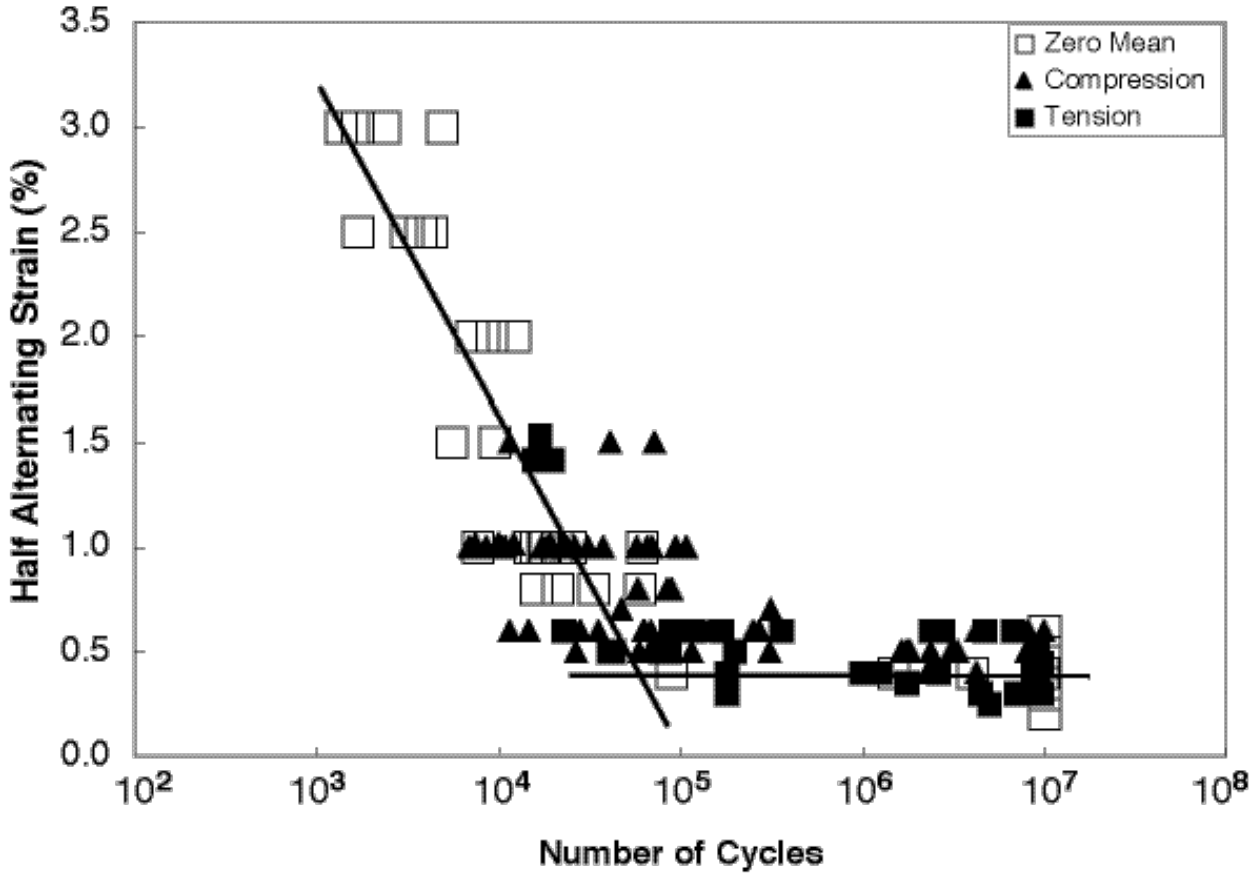

Figure 6: Fatigue data for conditions of tensile, compressive and zero-mean strains (-4% to +4%) for a range of cyclic amplitude.

Effects of Mean Strain

Samples were tested in both pull ("tension") and push ("compression") conditions to determine the effects of mean strain on fatigue life. These non-zero mean strain data are superimposed on the zero-meant strain data from Figure 4 and are plotted in Figure 6. In this figure, the data from tension tests are marked with closed square symbols and those samples cycled with compression forces are marked with closed triangles; the original zero-mean data are illustrated with open squares. Test conditions ranging from –4% to +4% mean strains and cyclic strains ranging from 0.2% to 1.5% are shown. None of the 10^7-cycle runout data are plotted in this figure. In general, it is difficult to differentiate the push and pull data from each other on this graph. Furthermore, the trendlines generated from the zero-mean conditions also appear to represent the average data for all conditions.

The fatigue life in linear-elastic engineering materials generally show a strong function of the mean stress. Increased mean stress decreases fatigue life for equivalent stress amplitude. These mean-stress effects can be better demonstrated with a constant life diagram, where the mean stress is plotted against the alternating stress for a fixed life. It is common to analyze these data with Goodman or Soderberg models to take both mean and alternating stress contributions into account for fatigue-safe designs [12]. Engineering safety factors can be easily calculated by comparing the mean and alternating stress conditions to their positions on the constant-life diagram.

The data from Figure 6 are graphed in a mean-strain *vs.* alternating-strain diagram, as shown in Figure 7. The 302 samples that survived 10^7 cycles under various mean and alternating strain conditions are also plotted as closed squares. It is immediately obvious that these data do not resemble either Soderberg or Goodman linear constant-life analysis. In contrast, the current "compressive" data indicate that there is no mean-strain effect up to -1.5%, which approximately corresponds to the strain for stress-induced martensite. The <u>increase</u> in fatigue life with increasing

strain is consistent with previous observations for Nitinol [9,11]. Furthermore, Kim and Miyazaki [5] observed that martensite has a longer fatigue life than austenite under identical rotary bend conditions. Moreover, fracture mechanics analyses [1, 2] demonstrated that Nitinol martensite has a lower fatigue crack growth rate than austenite. It is therefore possible that the observations of increased fatigue life can be explained in terms of the effects of the stress-induced martensitic transformation. Above about 2% mean strain the material is on the loading plateau and the applied deformation is accommodated by a martensitic transformation.

Fewer data were collected under mean "tension" conditions on the diamond samples, since these strain states are not experienced *in vivo* by stents or other similar Nitinol medical-device implants. Nevertheless, it is interesting to compare the behavior of the two test modes. At 1% tensile mean strain, the endurance limit is 0.25% cyclic strain, which is consistent with the values obtained for conditions of uniaxial tension of tube samples [8] and "pull" fatigue of laser-machined samples [9]. There were no fractures in the 22 specimens in the +3% to +4% mean-strain range at 0.25% to 0.4% cyclic strain, which indicates that there is increased life for the pull samples as well.

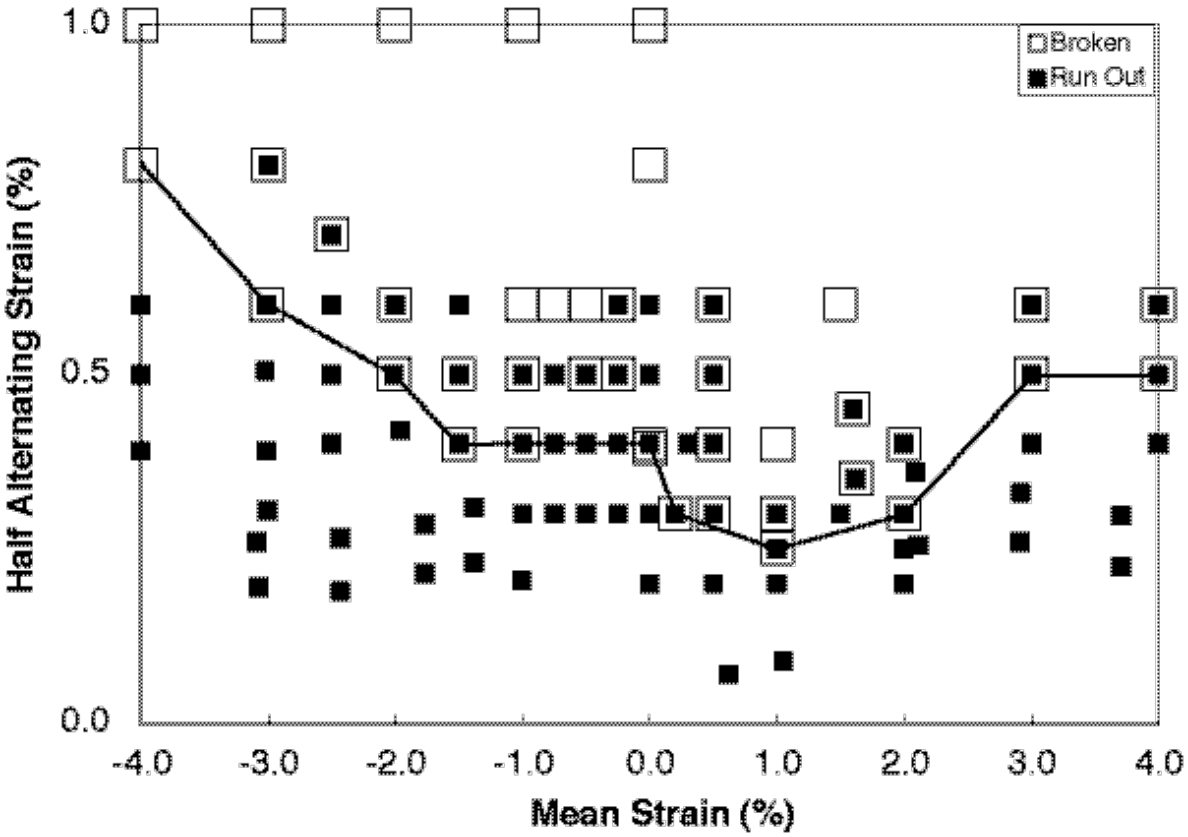

Figure 7: Constant life diagram of the fatigue data from Figure 6. Open square symbols indicate samples that failed in less than 10^7 cycles; filled square symbols indicate samples that survived. The line indicates the influence of mean strain on the endurance limit.

The present observations certainly indicate that fatigue life increase with increasing mean strain. The strong implication is that the stress-induced martensite is responsible for this behavior. It is not clear at the present time, however, if this is due, for example, to pure microstructural effects of martensite or perhaps to effects of the lower modulus in the stress-induced transformation regime. A lower modulus for the same deflection would result in a lower strain, which was not taken into account in the FEA model. Furthermore, there is also some merit to consider either a stress-based or a "strain energy" [19] approach to analyze the fatigue data. Preliminary analysis of the equivalent fatigue stresses also leads to the conclusion that the fatigue life increases in the martensitic region. Additional testing not reported here indicates that the stress and modulus decrease with increasing cyclic

deformation due to accumulation of microplasticity [18]. Additional testing of martensitic samples is underway to test these concepts.

SUMMARY

This report presents the preliminary results from Nitinol fatigue data collected on 432 diamond-shaped specimens that were cycled to a maximum life of 10^7 cycles. Low-cycle fatigue data from zero-mean strain conditions follow Coffin-Manson behavior with an exponent of –0.41. High-cycle data under these conditions indicate an endurance limit of 0.4% strain. SEM analysis of diamond samples under zero-mean conditions showed that failures occurred on the inside of the diamond arms, possibly due to non-uniform surface processing. The effects of mean strain were illustrated on a constant-life diagram and show that there is increased fatigue life at mean strains above about 1.5% compared with the zero-mean conditions. It was speculated that these effects could be due to strain accommodation from stress-induced martensitic transformation. It was also postulated that a strain energy approach may account for the effects of dynamic changes to stress and modulus.

REFERENCES

1. R. H. Dauskardt, T. W. Duerig, and R. O. Ritchie, MRS Int'l. Mtg. On Adv. Mats. **9** (1989), 243– 249.
2. A. L. McKelvey and R. O. Ritchie, Metallurgical and Materials Transactions, **32A** (2001) 731-743.
3. J. L. McNichols, Jr. and P. C. Brookes, J. Appl. Phys. **52**, no. 12 (1981) 7742–7444.
4. R.L. Holz, K. Sadananda, and M.A. Imam, Inter. J. of Fatigue **21** (1999) S137-S145.
5. Y. S. Kim and S. Miyazaki, in SMST-97: Proceedings of the Second International Conference on Shape Memory and Superelastic Technologies, eds. A.R. Pelton, *et al.* (Pacific Grove, California: International Organization on SMST, 1997), 473-478.
6. M. Reinhoehl, et al., in SMST-2000: Proceedings of the International Conference on Shape Memory and Superelastic Technologies, eds. S.M. Russell and A.R. Pelton, (Pacific Grove, California: International Organization on SMST, 2001) 397-403.
7. K. N. Melton and O. Mercier, Acta Metallurgica **27** (1979) 137–144.
8. R.M. Tabanli, N.K. Simha, and B.T. Berg, Mater. Sci. and Eng. A **273–275** (1999) 644-648.
9. D. Tolomeo, S. Davidson, and M. Santinoranont, in SMST-2000: Proceedings of the International Conference on Shape Memory and Superelastic Technologies, eds. S.M. Russell and A.R. Pelton, (Pacific Grove, California: International Organization on SMST, 2001) 471-476.
10. C. Kugler, D. Matson, and K. Perry, in SMST-2000: Proceedings of the International Conference on Shape Memory and Superelastic Technologies, eds. S.M. Russell and A.R. Pelton, (Pacific Grove, California: International Organization on SMST, 2001) 409-417.
11. W.J. Harrison and Z.C. Lin, in SMST-2000: Proceedings of the International Conference on Shape Memory and Superelastic Technologies, eds. S.M. Russell and A.R. Pelton, (Pacific Grove, California: International Organization on SMST, 2001) 391-396.
12. S. Subash, **Fatigue of Materials**, 2nd Ed., Cambridge University Press (1998).
13. X. Gong, J. Sheriff and A.R. Pelton, "Nitinol fatigue testing using a diamond shaped specimen", presented at SEM Annual Conference on Experimental and Applied Mechanics, Milwaukee, WI, June 2002.
14. N. Rebelo, M. Hsu, and H. Foadian, in SMST-2000: Proceedings of the International Conference on Shape Memory and Superelastic Technologies, eds. S.M. Russell and A.R. Pelton, (Pacific Grove, California: International Organization on SMST, 2001) 457-469.
15. N. Rebelo and M. Perry, Finite Element Analysis for the Design of Nitinol Medical Devices, Min. Invas. Ther. & Allied Technol. **9** (2) (2000) 75-80.
16. X. Gong and A.R. Pelton, "ABAQUS Analysis on Nitinol Medical Applications", ABAQUS Users' Conference, Newport, Rhode Island, May 2002, pp. 1 - 10.
17. X.-Y. Gong, A.R. Pelton, T.W. Duerig, N. Rebelo, and K.E. Perry, "Finite Element Analysis and Experimental Study on Superelastic Nitinol Stent", presented at the 14th US National Congress of Theoretical and Applied Mechanics, Blacksburg, VA, June 2002.
18. X.-Y. Gong, A.R. Pelton, unpublished results.
19. K.N. Smith, P. Watson and T.H. Topper, J. Materials **5** (1970) 767.